Geophysical Research Letters

RESEARCH LETTER
10.1029/2018GL078254

Key Points:
- We examine meridional variations in zonal mean isotope ratios of water vapor and precipitation within a steady state mass balance framework
- Patterns of evaporation and precipitation shape isotope ratios by varying the local drying ratio and effective distance to moisture sources
- Isotope ratios and precipitation amount are anticorrelated in zones where the local drying ratio dominates the atmospheric isotopic signal

Supporting Information:
- Supporting Information S1

Correspondence to:
A. Bailey,
abailey@ucar.edu

Citation:
Bailey, A., Posmentier, E., & Feng, X. (2018). Patterns of evaporation and precipitation drive global isotopic changes in atmospheric moisture. *Geophysical Research Letters*, *45*, 7093–7101. https://doi.org/10.1029/2018GL078254

Received 6 APR 2018
Accepted 27 JUN 2018
Accepted article online 5 JUL 2018
Published online 20 JUL 2018

Patterns of Evaporation and Precipitation Drive Global Isotopic Changes in Atmospheric Moisture

Adriana Bailey[1,2], Eric Posmentier[1], and Xiahong Feng[1]

[1]Department of Earth Sciences, Dartmouth College, Hanover, NH, USA, [2]Now at the National Center for Atmospheric Research, Boulder, CO, USA

Abstract Because water isotope ratios respond to phase changes during evaporation (*E*) and precipitation (*P*), they are candidate fingerprints of changing atmospheric hydrology. Moreover, through preservation in ice cores and other paleoproxies, they provide important insight into the past. Still, there is disagreement over what specific attributes of hydroclimate variability isotopes reveal. Here we argue that variations in zonal mean isotope ratios of water vapor and precipitation are largely a response to geographically shifting patterns of *E* and *P*. Differences in the relative importance of local versus remote changes in these moisture variables explain the apparent distinct isotopic sensitivities to temperature and precipitation amount in high and low latitudes, respectively. Not only does our work provide a unified framework for interpreting water isotopic measurements globally, but it also presents a novel approach for diagnosing water cycle changes in a warmer world.

Plain Language Summary Observations that track changes in the water cycle are critical for improving our understanding of the climate system. Particularly important are measurements that can verify whether imbalances in evaporation and precipitation increase in response to global warming. Because the isotope ratios of hydrogen and oxygen in water vapor and precipitation vary with rates of evaporation and precipitation, they are candidate fingerprints of water cycle changes. Here we use a simple mass balance model to evaluate the isotopic response of water vapor in the atmosphere to spatial variations in evaporation and precipitation. We find that these spatial patterns shape the isotope ratios by changing two critical factors: the efficiency with which precipitation dries the atmosphere and the probability that moisture is transported downwind (rather than rained out). These two factors suggest that isotope ratios are influenced both by local and by remote changes in evaporation and precipitation. Low-latitude isotope ratios respond largely to local imbalances in evaporation and precipitation, while high-latitude isotope ratios depend more on what happens "upstream." These findings provide key guidance for interpreting climate changes of the past and offer a novel approach for diagnosing water cycle changes in a warmer future.

1. Introduction

Thermodynamic arguments predict that regional imbalances in evaporation (*E*) and precipitation (*P*) enlarge (diminish) in response to increasing (decreasing) global temperature (Held & Soden, 2006). The isotope ratios of hydrogen (D/H) and oxygen ($^{18}O/^{16}O$) in water vapor and precipitation are potentially important diagnostics of such changes. Because of their distinct saturation vapor pressures, isotopically heavy water molecules (e.g., HDO and $H_2{}^{18}O$) preferentially condense, while isotopically light molecules (e.g., $H_2{}^{16}O$) preferentially evaporate. It is this sensitivity to phase changes that suggests isotope ratios might trace shifting imbalances in *E* and *P* in a changing climate (Bailey et al., 2017). Furthermore, because the isotopic signal of precipitation is transferred to paleoproxies, such as ice cores and speleothems (e.g., Dee et al., 2015), isotope ratios are one of a limited number of constraints on hydroclimate variability before the instrumental period. However, their use poses a classic geochemical inverse problem, and so a method for extracting quantitative global information about shifts in hydrologic balance from isotopic records is needed.

Historically, isotopic variations in low latitudes have been interpreted as an indicator of changing local precipitation amount, while variations in high latitudes have been considered a reflection of changing temperature (e.g., Dansgaard, 1964; Johnsen et al., 1989, 1995; Lorius & Merlivat, 1977; Masson-Delmotte et al., 2008; Niedermeyer et al., 2010; Rozanski et al., 1993; Tierney et al., 2008). Yet empirically derived relationships between isotopes and local meteorological variables of interest vary widely geographically and have

proven insufficient for describing isotopic variability at many locations (Aggarwal et al., 2012; Boyle, 1997; Conroy et al., 2013; Fisher et al., 2004; Krinner et al., 1997; Kurita et al., 2009; Masson-Delmotte et al., 2008; Sime et al., 2009; Sodemann et al., 2008; Sturm et al., 2010). Indeed, precipitation and ice cores in Alaska sometimes show stronger correlations between water isotope ratios and moisture source region than temperature (Fisher et al., 2004; Putman et al., 2017), and modern precipitation measurements in the tropical Pacific suggest that isotope ratios respond more sensitively to variations in the intensity and organization of convection regionally than to the amount of local precipitation (Conroy et al., 2016; Kurita, 2013; Kurita et al., 2009; Moerman et al., 2013). More recently, studies have shown correlations between isotope ratios and regional imbalances in E and P (Feng et al., 2009; Lee et al., 2007; Moore et al., 2014) or associated variations in atmospheric residence time and moisture transport (Aggarwal et al., 2012; Bailey et al., 2017; Putman et al., 2017). Nevertheless, to decipher changes in hydrologic balance from isotope ratios, a strong theoretical framework that can explain these correlations is necessary.

The incorporation of water isotopic tracers in state-of-the-art general circulation models (GCMs; Galewsky et al., 2016; Sturm et al., 2010, and references therein) has created new opportunities to evaluate isotopic responses to a broad suite of large- and small-scale hydrological perturbations (e.g., Bailey et al., 2017; Bony et al., 2008; Caley et al., 2014; Hurley et al., 2012; Noone & Simmonds, 2002; Risi et al., 2008; Sutanto et al., 2015; Wright et al., 2009). Yet because of the complexity of these models, and their difficulties in representing evaporation and precipitation accurately (Nusbaumer et al., 2017), GCMs are not necessarily ideal for elucidating the sensitivity of isotope ratios to variations in E and P. In contrast, zonal models offer a vastly simpler framework for evaluating isotopic sensitivities to the integrated effects of atmospheric moisture removal and recharge (Fisher, 1990; Hendricks et al., 2000; Kavanaugh & Cuffey, 2003; Noone, 2008). Such models have proven useful for testing isotopic responses to local and remote variations in climate. They have demonstrated, for instance, that high-latitude isotope ratios incorporate information about lower-latitude temperature changes, with distillation along the moisture pathway influencing the strength of the low-latitude signal.

Here we use the zonal model framework and principles of mass balance to simulate the isotopic response to meridional shifts in E and P. This simple design allows us to evaluate latitudinal differences in the sensitivity of isotope ratios to local and remote changes in hydrologic balance. The approach provides a consistent methodology for integrated interpretation of isotope ratios in low- and high-latitude environments. Moreover, it identifies key features of *global* hydroclimate variability that isotope ratios in water vapor and precipitation uniquely reveal, providing a new lens for examining current and past hydrological change.

2. A One-Dimensional Steady State Mass Balance Model

To test whether water isotope ratios are robust indicators of changes in hydrologic balance, we construct a one-dimensional (1-D) steady state model that resolves the volume-averaged climate in 36 zones of 5° latitude (index $i = 1 \ldots 36$ from south to north). Zonal mean E and P are the only specified variables. Estimates of E and P for December, January, February and June, July, August are obtained from an isotopically enabled version of the National Center for Atmospheric Research's Community Atmosphere Model (CAM) version 5 (i.e., isoCAM; Nusbaumer et al., 2017; supporting information). The moisture fluxes simulated by isoCAM ($kg{\cdot}m^{-2}{\cdot}year^{-1}$) are converted to mass flow rates (kg/year) by accounting for differences in area among zonal bands.

Defining F_i as the northward mass flow of water (kg/year) across the boundary between zones i and $i + 1$, conservation of mass for the ith zone in steady state requires that

$$F_{i-1} - F_i + E_i - P_i = 0, \tag{1}$$

where the difference in northward atmospheric transport ($F_{i-1} - F_i$) represents moisture convergence.

Mass conservation for an individual isotope can be derived by multiplying each total water flow by its appropriate isotopic composition:

$$\delta_{i-1}F_{i-1} - \delta_i F_i + (-10)E_i - (\delta_i + 10)P_i = 0. \tag{2}$$

Here the isotopic composition of evaporation is assumed fixed at −10‰ and the isotopic composition of precipitation is offset +10‰ from the zone's water vapor isotope ratio. Throughout the paper δ will be evaluated

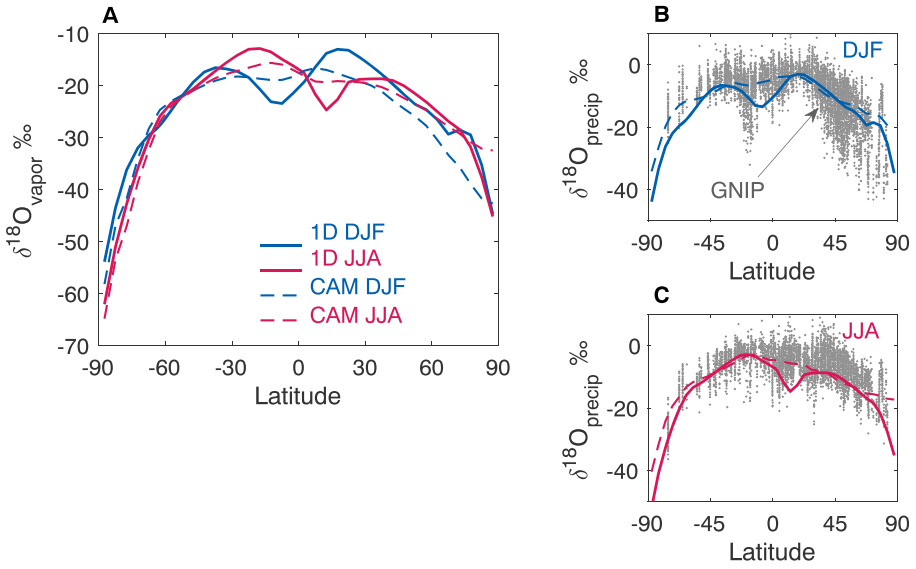

Figure 1. Zonal mean isotopic climatologies simulated by the one-dimensional steady state mass balance model compared to (a) simulated water vapor isotope ratios from an isotopically enabled version of CAM5 (i.e., isoCAM, dashed lines) and to (b) and (c) precipitation isotope ratios simulated (isoCAM) and observed (Global Network of Isotopes in Precipitation, gray dots). Climatologies are shown separately for DJF (blue) and JJA (red). 1D = one-dimensional; CAM = Community Atmosphere Model; DJF = December, January, February; JJA = June, July, August; GNIP = Global Network of Isotopes in Precipitation.

exclusively as the oxygen isotope ratio of water vapor expressed in conventional delta notation (supporting information).

Equation (2) is strictly valid only for $F_{i\text{-}1}, F_i \geq 0$. If either F is negative, the subscript of the corresponding δ must be incremented by 1. With this exception, the assumptions incorporated into equation (2) may be summarized as follows:

1. Sea surface water has an oxygen isotope ratio of 0‰.
2. Sea surface evaporative fractionation for oxygen is 10‰.
3. Fractionation during condensation is 10‰ (cf. Lee et al., 2007).

By adopting these assumptions, the model does not consider any direct effects of temperature, relative humidity, or wind speed on the isotope ratio of water vapor evaporated from the sea surface. Furthermore, it ignores the dependence of isotopic fractionation on temperature during condensation.

With only E and P as inputs, the 1-D steady state mass balance model broadly reproduces the key meridional variations in isotope ratios observed in the Global Network of Isotopes in Precipitation (International Atomic Energy Agency/World Meteorological Organization, 2018; supporting information) and simulated in isoCAM (Figure 1), thus validating the mass balance approach. Water vapor and precipitation isotope ratios decrease with latitude, except near the equator, where deep convection within the Intertropical Convergence Zone (ITCZ) depletes the atmosphere of isotopically heavy water locally. This area of localized depletion shifts between hemispheres as the ITCZ migrates annually. Interestingly, isotopic variations associated with the ITCZ are stronger in the 1-D simulation than in the GCM. In this respect, they better represent the range of tropical isotope ratios observed, particularly during December, January, February (Figure 1b). The GCM, in contrast, resolves vertical circulations, which transport isotopically enriched moisture across the equator at low altitudes while returning isotopically depleted moisture aloft. Such a circulation plausibly diminishes low-latitude, total-column isotopic differences between hemispheres.

Localized depletion associated with the ITCZ is also consistent with the so-called "amount effect"—a negative correlation between water isotope ratios and precipitation frequently invoked in the interpretation of paleoproxies (e.g., Cruz et al., 2005; Niedermeyer et al., 2010; Sano et al., 2012; Tierney et al., 2008) (Figure 2a). Although this anticorrelation broadly characterizes the tropics (Dansgaard, 1964), its absence in many locations has motivated investigations into whether factors other than precipitation amount influence this

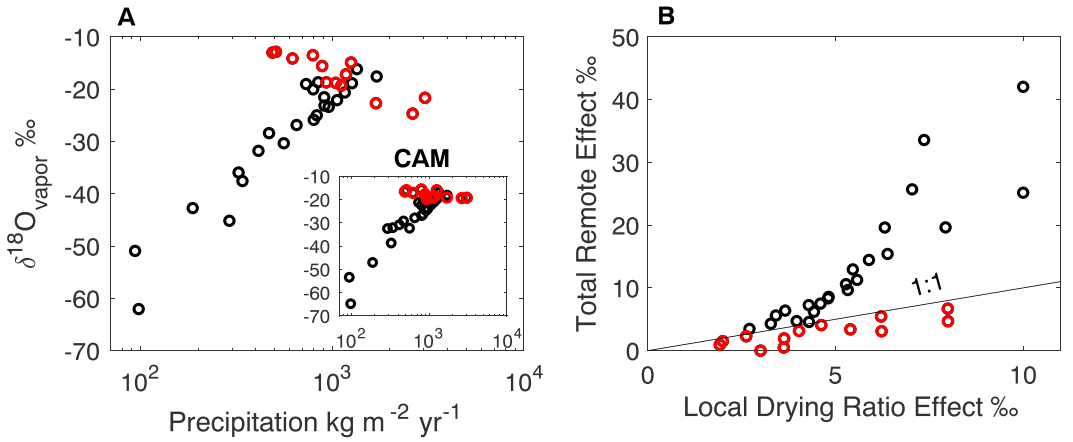

Figure 2. The so-called "amount effect" (a) appears in the one-dimensional simulation as a negative correlation between water vapor isotope ratios and precipitation amount (i.e., flux in kg·m^{-2}·year^{-1}) in zones equatorward of 40° (red circles). Zones poleward of 40° are shown with black circles. Results from isoCAM are shown for comparison (insert). (b) This relationship emerges in zones where the isotopic influence of the local drying ratio is much stronger than the combined influence of drying ratios elsewhere (i.e., remote effects; see section 3). Results are shown for June, July, August only.

relationship. These factors have included the height—hence, condensation temperature (Scholl et al., 2009)—of clouds, the mesoscale organization of convection, (Aggarwal et al., 2016; Kurita, 2013), the degree of rain evaporation within downdrafts (Kurita, 2013; Risi et al., 2008), and the magnitude and altitude of moisture convergence (Moore et al., 2014; Torri et al., 2017). The fact that our 1-D simulation reproduces an amount effect using only principles of mass balance suggests an important role for evaporation—not just precipitation—in setting tropical isotope ratios.

3. Local Versus Remote Hydrological Changes

As the difference between E and P in a zone i increases, hydrologic balance necessitates that moisture transport readjust (equation (1)), requiring changes in E-P elsewhere. Since shifts in the relative balance of E and P influence the isotopic composition of water vapor locally (equation (2)), changes in hydrologic balance upwind of zone i must influence the isotopic composition of moisture transported into i. Consequently, isotopic records at any single location need not represent *local* changes in hydrologic balance.

This point is readily illustrated using a simple idealized simulation in which E and P are set equal everywhere except in two zones: an evaporative source region and a precipitation sink region (Figure 3). A large positive isotopic anomaly emerges locally where $E/P > 1$ and a large negative anomaly where $E/P < 1$. However, isotopic enrichment also occurs immediately downwind of the source region, even though local moisture supply (E) and demand (P) remain balanced. In these downwind regions, the isotope ratios increase due to horizontal transport.

Given a more realistic hydrologic circulation, the exact dependence of the water vapor isotope ratio on both local and remote imbalances in E and P can be calculated from equation (2) by redefining the isotopic convergence ($\delta_{i\text{-}1}F_{i\text{-}1} - \delta_i F_i$) as the difference between flows into and out of each zone ($\delta_{\text{in},i}F_{\text{in},i} - \delta_{\text{out},i}F_{\text{out},i}$). In this reformulation, flow entering zone i ($F_{\text{in},i}$) is, by definition, always positive regardless of the direction of transport. The $\delta_{\text{in},i}$ is the δ of the zone immediately upwind (e.g., δ_{i+1} for southward and δ_{i-1} for northward transport). The reformulated version of equation (2) takes on more obvious meaning by incorporating two new variables, the drying ratio (D^*) and the remote fraction (R^*). The former describes the efficacy with which P dries the atmosphere (e.g., Smith & Evans, 2007), while the latter quantifies the proportion of moisture gained through transport:

$$D_i^* = P_i/\left(E_i + F_{\text{in},i}\right), \tag{3}$$

$$R_i^* = F_{\text{in},i}/\left(E_i + F_{\text{in},i}\right). \tag{4}$$

The water vapor isotope ratio for zone i is then

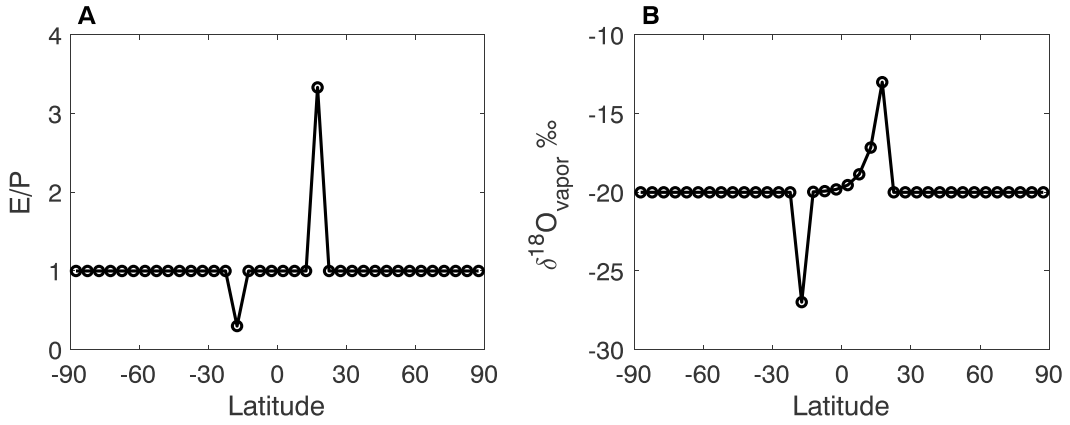

Figure 3. An idealized experiment in which (a) perturbations in *E* and *P* create an evaporative source region centered at 17.5°N and a precipitation sink region centered at 17.5°S, linked by a southward atmospheric moisture flow. (b) Water vapor isotope ratios are enriched not only where $E/P > 1$ but also in zones downwind due to horizontal transport. *E* = evaporation; *P* = precipitation.

$$\delta_i = -10 - 10D_i^* - \left(-10 - \delta_{\mathrm{in},i}\right)R_i^*, \tag{5}$$

which, solved recursively, yields

$$\delta_i = -10\left(1 + D_i^* + \theta_i \Sigma_{n=1}^{N} D_{i+n}^* \Pi_{m=1}^{n} R_{i-1+m}^* + (1-\theta_i)\Sigma_{s=1}^{S} D_{i-s}^* \Pi_{r=1}^{s} R_{i+1-r}^*\right). \tag{6}$$

N and *S* are the total numbers of zones to the north and south, respectively, that contribute moisture to zone *i*, and θ is a weighting function that defines the relative contribution of northerly moisture transport to R^*. In our simulations, θ is either 0 or 1 for all but a single tropical zone. Thus, if zone *i* receives moisture from three neighboring zones to the south, its isotope ratio is given by

$$\delta_i = -10\left(1 + D_i^* + D_{i-1}^* R_i^* + D_{i-2}^* R_i^* R_{i-1}^* + D_{i-3}^* R_i^* R_{i-1}^* R_{i-2}^*\right). \tag{7}$$

This formulation not only demonstrates the existence of isotopic teleconnections (i.e., *remote effects*)—which have been documented previously (Cuffey, 2000; Fisher, 1990; Hendricks et al., 2000; Noone, 2008; Noone & Simmonds, 2002)—but also reveals that the quantitative contribution of each remote zone is proportional to its drying ratio. This contribution may be more or less attenuated depending upon the characteristics of atmospheric transport. Namely, the compound effects of R^* along the moisture pathway represent the probability that evaporation from a remote zone will reach zone *i* (cf. Fisher's "survival distance" function; Fisher, 1990).

Equation (6) provides critical insight into why precipitation isotope ratios in the tropics broadly correlate with local precipitation amount. In tropical regions, the local drying ratio is often larger than the probability-weighted sum of drying ratios upwind, either because the fractional contribution of moisture from remote sources is small (e.g., subtropics) or because moisture is sourced from subtropical regions where D^* approaches 0 (e.g., deep tropics; Figure 4). Consequently, local hydrological effects dominate remote effects in shaping the isotope ratios of water vapor and precipitation (Figure 2b). Since greater *P* causes D^* to increase, and δ is negatively correlated with D^* (equation (5)), a negative correlation between local precipitation and isotope ratios emerges (Figure 2a).

In comparison, higher latitudes depend not only on a larger proportion of remote moisture but also on moisture from regions with higher drying ratios (Figure 4). Energy constraints ultimately influence both factors, which is why high-latitude isotope ratios tend to correlate with temperature (i.e., the *temperature effect*; Dansgaard, 1964). Indeed, because low temperature reduces the energy available for evaporation and lowers the atmosphere's moisture-holding capacity, both *E* and *P* decrease toward the poles. However, since moisture transported poleward is much less decremented by low temperatures, *E* decreases relative to *P* while the remote fraction (R^*) increases (Figure 4a). Eventually, reductions in *E* sufficiently limit the moisture available

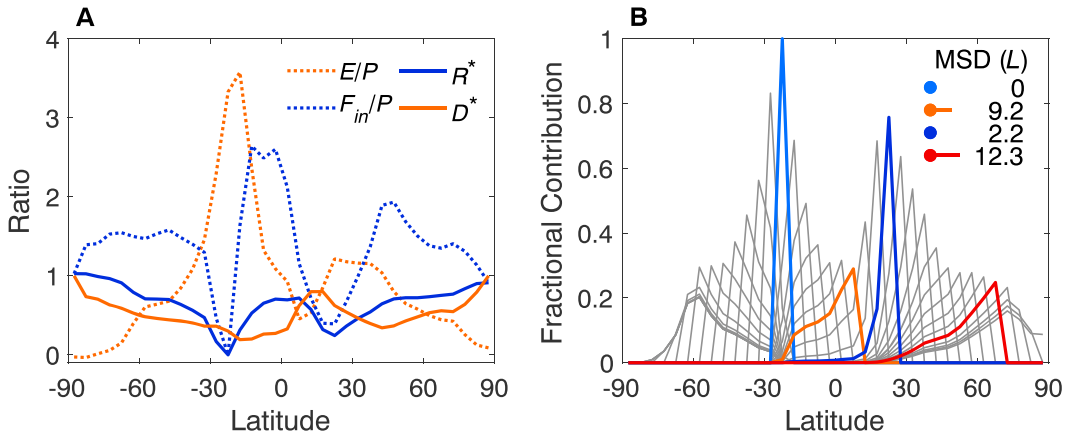

Figure 4. Latitudinal variations in drying ratio (D^*), remote fraction (R^*), and mean source distance (L). (a) D^* (orange) and R^* (blue) are plotted alongside E/P (dotted orange) and F_{in}/P (dotted blue) as a function of latitude. (b) Frequency distributions show the geographic distribution of source regions for each modeled zone and indicate their fractional moisture contributions. In the tropics and midlatitudes, the largest fraction of moisture gained is locally evaporated. A case in point is the bright blue curve, which equals 1 in the zonal band 25–30°S and 0 elsewhere, indicating that 100% of moisture gained is local E. Mean source distances are shown to scale and reported in degrees latitude for the four highlighted distributions. Results are shown for June, July, August only. E = evaporation; P = precipitation; F_{in} = moisture gained by transport; MSD = mean source distance.

for transport so that F_{in} also decreases relative to P. This enlarges the drying ratio (D^*, equation (3)), and, together, larger D^* and R^* lower the isotope ratio at cold temperatures.

4. Mean Moisture Source Distances

As E/P decreases poleward, the remote fraction must increase to provide moisture. This requires that the mean source distance—or mean distance moisture travels from evaporative source regions to a zone of interest—increase (Figure 4b). Since each *remote* term in equation (6) scales nearly linearly with mean source distance (supporting information), the latter provides a compact and close approximation for remote hydrological effects on the water vapor isotope ratio. Linearly combining information about the local drying ratio (D^*) and mean source distance (L, i.e., a length scale) in the form

$$\delta = \beta_0 + \beta_1 D^* + \beta_2 L, \tag{8}$$

thus robustly reproduces the meridional variations in zonal mean isotope ratios simulated by the 1-D model (Figure 5a) without needing to distinguish tropical versus high-latitude regions. A least squares fit for June, July, August produces values of −6.19‰ (−7.78‰, −4.61‰), −15.00‰ (−18.96‰, −11.04‰), and −1.09‰ per degree latitude (−1.19‰ per degree latitude, −0.99‰ per degree latitude) for β_0, β_1, and β_2, respectively, with 95% confidence intervals reported parenthetically.

A prominent outcome of this linear approximation is that it allows one to predict water isotope ratios from just two state variables. Moreover, coefficients β_1 and β_2 accurately predict isotopic changes with time on interseasonal timescales (Figure 5b). This result contrasts with the different spatial versus temporal sensitivities of isotope ratios to temperature observed and modeled at high latitudes (e.g., Jouzel et al., 1997).

5. Implications

The demonstrated dependence of isotope ratios on local *and* remote imbalances in E and P has important implications for interpretation of isotopic records. After all, the degree to which individual ice cores and speleothems record local versus nonlocal climatic changes has long been a question of interest (e.g., Caley et al., 2014; Cheng et al., 2012; Fisher et al., 2004; Goldsmith et al., 2017; Masson-Delmotte et al., 2008; Pausata et al., 2011). Our analysis provides a framework for understanding why paleoproxies distant in space can share strong isotopic signals while those nearby may not. The outcome depends both on the

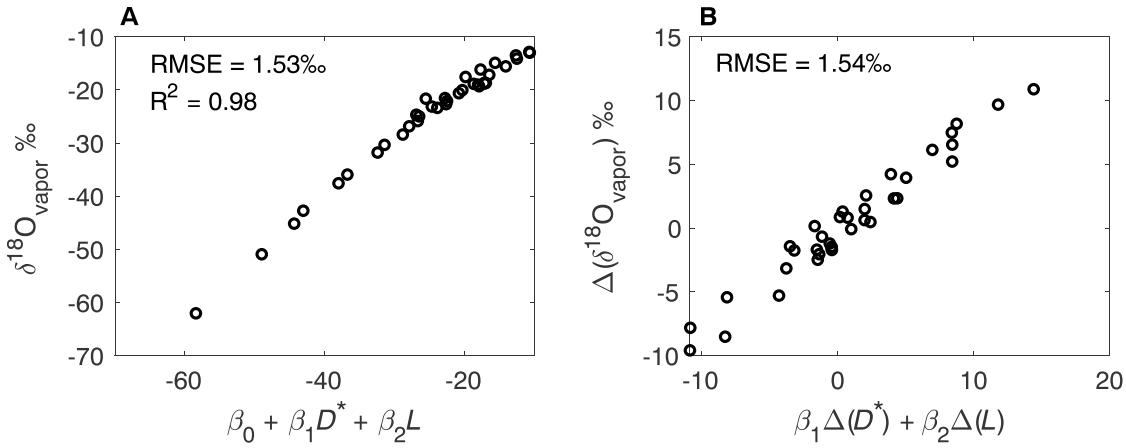

Figure 5. A linear combination of drying ratio (D^*) and mean source distance (L) accurately reproduces (a) spatial variations in water vapor isotope ratios simulated by the one-dimensional model for the June, July, August season. Both the RMSE and the R^2 value are shown. (b) The same regression coefficients shown in (a) predict seasonal differences (December, January, February-June, July, August) in zonal mean isotope ratios with comparable low error. RMSE = root-mean-square error.

nature of local hydrological perturbations and on the strength of regional linkages through the atmospheric circulation.

Consistent with previous findings (e.g., Hendricks et al., 2000), our results suggest that high-latitude isotope ratios will tend to reveal more about changing moisture transport than local meteorology, while the opposite should be true at latitudes equatorward of ~40° (Figure 2b). Nevertheless, to truly disentangle these factors, isotopic records from a single location will be insufficient. Instead, data from a spatially broad network of measurements, such as the Global Network of Isotopes in Precipitation, need to be analyzed for their spatial distributions. These spatial patterns should be examined in the context of forward modeling approaches, such as demonstrated here and advocated previously (Sturm et al., 2010). In the absence of such spatial coverage, additional tracers will be necessary to constrain either the drying ratio or mean source distance at the site of the individual isotopic record. Over the recent instrumental period, in situ or remote estimates of E, P, and F_{in} may allow one to calculate the drying ratio, so that changes in mean source distance can be extracted from isotopic measurements. Paleoclimate analyses, on the other hand, will require a second tracer—sensitive either to precipitation processes or transport distance—that is also preserved in the proxy record.

As global temperatures continue to rise, broad networks of water vapor and precipitation isotopic measurements can be used to answer several pressing questions about current hydroclimate change, including (1) whether the efficiency with which precipitation dries the atmosphere is decreasing, resulting in longer moisture residence times in the atmosphere (cf. Aggarwal et al., 2012), (2) whether distances between moisture sources and sinks are lengthening in response to longer residence times (Singh et al., 2016), and (3) whether, contrastingly, mean moisture source distances for some regions are shortening in response to the Hadley cell expanding poleward (Collins et al., 2013). The ability to distinguish and quantify these trends has key implications for predicting future climate.

Acknowledgments
The authors thank K. Cuffey and a second reviewer for their constructive critiques of this work. A. Bailey was supported by the Joseph P. Obering Fellowship from Dartmouth College's Department of Earth Sciences. The National Center for Atmospheric Research is sponsored by the National Science Foundation. Data sources are described in the supporting information.

References

Aggarwal, P. K., Alduchov, O. A., Froehlich, K. O., Araguas-Araguas, L. J., Sturchio, N. C., & Kurita, N. (2012). Stable isotopes in global precipitation: A unified interpretation based on atmospheric moisture residence time. *Geophysical Research Letters*, *39*, L11705. https://doi.org/10.1029/2012GL051937

Aggarwal, P. K., Romatschke, U., Araguas-Araguas, L., Belachew, D., Longstaffe, F. J., Berg, P., et al. (2016). Proportions of convective and stratiform precipitation revealed in water isotope ratios. *Nature Geoscience*, *9*(8), 624–629. https://doi.org/10.1038/ngeo2739

Bailey, A., Blossey, P. N., Noone, D., Nusbaumer, J., & Wood, R. (2017). Detecting shifts in tropical moisture imbalances with satellite-derived isotope ratios in water vapor. *Journal of Geophysical Research: Atmospheres*, *122*, 5763–5779. https://doi.org/10.1002/2016JD026222

Bony, S., Risi, C., & Vimeux, F. (2008). Influence of convective processes on the isotopic composition (δ^{18}O and δD) of precipitation and water vapor in the tropics: 1. Radiative-convective equilibrium and tropical ocean–global atmosphere–coupled ocean-atmosphere response experiment (TOGA-COARE) simulations. *Journal of Geophysical Research*, *113*, D19305. https://doi.org/10.1029/2008JD009942

Boyle, E. A. (1997). Cool tropical temperatures shift the global δ^{18}O-T relationship: An explanation for the ice core δ^{18}O-borehole thermometry conflict? *Geophysical Research Letters*, *24*(3), 273–276. https://doi.org/10.1029/97GL00081

Caley, T., Roche, D. M., & Renssen, H. (2014). Orbital Asian summer monsoon dynamics revealed using an isotope-enabled global climate model. *Nature Communications*, *5*(1), 5371. https://doi.org/10.1038/ncomms6371

Cheng, H., Sinha, A., Wang, X., Cruz, F. W., & Lawrence Edwards, R. (2012). The global paleomonsoon as seen through speleothem records from Asia and the Americas. *Climate Dynamics*, *39*(5), 1045–1062. https://doi.org/10.1007/s00382-012-1363-7

Collins, M., Knutti, R., Arblaster, J., Dufresne, J.-L., Fichefet, T., Friedlingstein, P., et al. (2013). Long-term climate change: Projections, commitments and irreversibility. In T. F. Stocker, et al. (Eds.), *Climate change 2013: The physical science basis. Contribution of Working Group I to the Fifth Assessment Report of the Intergovernmental Panel on Climate Change* (pp. 1029–1136). Cambridge, United Kingdom and New York, NY: Cambridge University Press.

Conroy, J. L., Cobb, K. M., & Noone, D. (2013). Comparison of precipitation isotope variability across the tropical Pacific in observations and SWING2 model simulations. *Journal of Geophysical Research: Atmospheres*, *118*, 5867–5892. https://doi.org/10.1002/jgrd.50412

Conroy, J. L., Noone, D., Cobb, K. M., Moerman, J. W., & Konecky, B. L. (2016). Paired stable isotopologues in precipitation and vapor: A case study within western tropical Pacific storms. *Journal of Geophysical Research: Atmospheres*, *121*(7), 3290–3303. https://doi.org/10.1002/2015JD023844

Cruz, F. W. Jr., Burns, S. J., Karmann, I., Sharp, W. D., Vuille, M., Cardoso, A. O., et al. (2005). Insolation-driven changes in atmospheric circulation over the past 116,000 years in subtropical Brazil. *Nature*, *434*(7029), 63–66. https://doi.org/10.1038/nature03365

Cuffey, K. M. (2000). Methodology for use of isotopic climate forcings in ice sheet models. *Geophysical Research Letters*, *27*(19), 3065–3068. https://doi.org/10.1029/2000GL011756

Dansgaard, W. (1964). Stable isotopes in precipitation. *Tellus*, *16*(4), 436–468. https://doi.org/10.1111/j.2153-3490.1964.tb00181.x.

Dee, S., Emile-Geay, J., Evans, M. N., Allam, A., Steig, E. J., & Thompson, D. (2015). PRYSM: An open-source framework for PRoxY System Modeling, with applications to oxygen-isotope systems. *Journal of Advances in Modeling Earth Systems*, *7*(3), 1220–1247. https://doi.org/10.1002/2015MS000447

Feng, X., Faiia, A. M., & Posmentier, E. S. (2009). Seasonality of isotopes in precipitation: A global perspective. *Journal of Geophysical Research*, *114*, D08116. https://doi.org/10.1029/2008JD011279

Fisher, D. A. (1990). A zonally-averaged stable-isotope model coupled to a regional variable-elevation stable-isotope model. *Annals of Glaciology*, *14*, 65–71. https://doi.org/10.1017/S0260305500008284

Fisher, D. A., Wake, C., Kreutz, K., Yalcin, K., Steig, E., Mayewski, P., et al. (2004). Stable isotope records from Mount Logan, eclipse ice cores and nearby Jellybean Lake. Water cycle of the North Pacific over 2000 years and over five vertical kilometres: Sudden shifts and tropical connections. *Géographie Physique et Quaternaire*, *58*(2–3), 337–352. https://doi.org/10.7202/013147ar

Galewsky, J., Steen-Larsen, H. C., Field, R. D., Worden, J., Risi, C., & Schneider, M. (2016). Stable isotopes in atmospheric water vapor and applications to the hydrologic cycle. *Reviews of Geophysics*, *54*, 809–865. https://doi.org/10.1002/2015RG000512

Goldsmith, Y., Broecker, W. S., Xu, H., Polissar, P. J., deMenocal, P. B., Porat, N., et al. (2017). Northward extent of East Asian monsoon covaries with intensity on oribital and millennial timescales. *Proceedings of the National Academy of Sciences*, *114*(8), 1817–1821. https://doi.org/10.1073/pnas.1616708114

Held, I. M., & Soden, B. J. (2006). Robust responses of the hydrological cycle to global warming. *Journal of Climate*, *19*(21), 5686–5699. https://doi.org/10.1175/JCLI3990.1

Hendricks, M. B., DePaolo, D. J., & Cohen, R. C. (2000). Space and time variation of $\delta^{18}O$ and δD in precipitation: Can paleotemperature be estimated from ice cores? *Global Biogeochemical Cycles*, *14*(3), 851–861. https://doi.org/10.1029/1999GB001198

Hurley, J. V., Galewsky, J., Worden, J., & Noone, D. (2012). A test of the advection-condensation model for subtropical water vapor using stable isotopologue observations from Mauna Loa Observatory, Hawaii. *Journal of Geophysical Research*, *117*, D19118. https://doi.org/10.1029/2012JD018029

International Atomic Energy Agency/World Meteorological Organization (2018). Global Network of Isotopes in Precipitation, The GNIP Database, accessible at: http://www.iaea.org/water

Johnsen, S. J., Dahl-Jensen, D., Dansgaard, W., & Gundestrup, N. (1995). Greenland palaeotemperatures derived from GRIP bore hole temperature and ice core isotope profiles. *Tellus B*, *47*(5), 624–629. https://doi.org/10.3402/tellusb.v47i5.16077

Johnsen, S. J., Dansgaard, W., & White, J. W. C. (1989). The origin of Arctic precipitation under present and glacial conditions. *Tellus B*, *41*(4), 452–468. https://doi.org/10.3402/tellusb.v41i4.15100

Jouzel, J., Alley, R. B., Cuffey, K. M., Dansgaard, W., Grootes, P., Hoffmann, G., et al. (1997). Validity of the temperature reconstruction from water isotopes in ice cores. *Journal of Geophysical Research*, *102*(C12), 26,471–26,487. https://doi.org/10.1029/97JC01283

Kavanaugh, J. L., & Cuffey, K. M. (2003). Space and time variation of $\delta^{18}O$ and δD in Antarctic precipitation revisited. *Global Biogeochemical Cycles*, *17*(1), 1017. https://doi.org/10.1029/2002GB001910

Krinner, G., Genthon, C., & Jouzel, J. (1997). GCM analysis of local influences on ice core δ signals. *Geophysical Research Letters*, *24*(22), 2825–2828. https://doi.org/10.1029/97GL52891

Kurita, N. (2013). Water isotopic variability in response to mesoscale convective system over the tropical ocean. *Journal of Geophysical Research: Atmospheres*, *118*, 10,376–10,390. https://doi.org/10.1002/jgrd.50754

Kurita, N., Ichiyanagi, K., Matsumoto, J., Yamanaka, M. D., & Ohata, T. (2009). The relationship between the isotopic content of precipitation and the precipitation amount in tropical regions. *Journal of Geochemical Exploration*, *102*(3), 113–122. https://doi.org/10.1016/j.gexplo.2009.03.002

Lee, J.-E., Fung, I., DePaolo, D. J., & Henning, C. C. (2007). Analysis of the global distribution of water isotopes using the NCAR atmospheric general circulation model. *Journal of Geophysical Research*, *112*, D16306. https://doi.org/10.1029/2006JD007657

Lorius, C., & Merlivat, L. (1977). Distribution of mean surface stable isotope values in East Antarctica: Observed changes with depth in the coastal area. In *Isotopes and impurities in snow and ice:: Proceedings of the Grenoble Symposium*, August–September 1975. International Association of Hydrological Sciences Publication No. 118 (pp. 127–137). http://hydrologie.org/redbooks/a118/iahs_118_0127.pdf

Masson-Delmotte, V., Hou, S., Ekaykin, A., Jouzel, J., Aristarain, A., Bernardo, R. T., et al. (2008). A review of Antarctic surface snow isotopic composition: Observations, atmospheric circulation, and isotopic modeling. *Journal of Climate*, *21*(13), 3359–3387. https://doi.org/10.1175/2007JCLI2139.1

Moerman, J. W., Cobb, K. M., Adkins, J. F., Sodemann, H., Clark, B., & Tuen, A. A. (2013). Diurnal to interannual rainfall $\delta^{18}O$ variations in northern Borneo driven by regional hydrology. *Earth and Planetary Science Letters*, *369-370*, 108–119. https://doi.org/10.1016/j.epsl.2013.03.014

Moore, M., Kuang, Z., & Blossey, P. N. (2014). A moisture budget perspective of the amount effect. *Geophysical Research Letters*, *41*, 1329–1335. https://doi.org/10.1002/2013GL058302

Niedermeyer, E. M., Schefuß, E., Sessions, A. L., Mulitza, S., Mollenhauer, G., Schulz, M., & Wefer, G. (2010). Orbital- and millennial-scale changes in the hydrologic cycle and vegetation in the western African Sahel: Insights from individual plant wax δD and $\delta^{13}C$. *Quaternary Science Reviews*, *29*(23–24), 2996–3005. https://doi.org/10.1016/j.quascirev.2010.06.039

Noone, D. (2008). The influence of midlatitude and tropical overturning circulation on the isotopic composition of atmospheric water vapor and Antarctic precipitation. *Journal of Geophysical Research*, *113*, D04102. https://doi.org/10.1029/2007JD008892

Noone, D., & Simmonds, I. (2002). Annular variations in moisture transport mechanisms and the abundance of $\delta^{18}O$ in Antarctic snow. *Journal of Geophysical Research*, *107*(D24), 4742. https://doi.org/10.1029/2002JD002262

Nusbaumer, J., Wong, T., Bardeen, C., & Noone, D. (2017). Evaluating hydrological processes in the Community Atmosphere Model version 5 (CAM5) using stable isotope ratios of water. *Journal of Advances in Modeling Earth Systems*, *9*(2), 949–977. https://doi.org/10.1002/2016MS000839

Pausata, F. S., Battisti, D. S., Nisancioglu, K. H., & Bitz, C. M. (2011). Chinese stalagmite $\delta^{18}O$ controlled by changes in the Indian monsoon during a simulated Heinrich event. *Nature Geoscience*, *4*(7), 474–480. https://doi.org/10.1038/NGEO1169

Putman, A. L., Feng, X., Sonder, L. J., & Posmentier, E. S. (2017). Annual variation in event-scale precipitation $\delta^{2}H$ at Barrow, AK, reflects vapor source region. *Atmospheric Chemistry and Physics*, *17*(7), 4627–4639. https://doi.org/10.5194/acp-17-4627-2017

Risi, C., Bony, S., & Vimeux, F. (2008). Influence of convection processes on the isotopic composition ($\delta^{18}O$ and δD) of precipitation and water vapor in the tropics: 2. Physical interpretation of the amount effect. *Journal of Geophysical Research*, *113*, D19306. https://doi.org/10.1029/2008JD009943

Rozanski, K., Araguás-Araguás, L., & Gonfiantini, R. (1993). Isotopic patterns in modern global precipitation. In R. Swart, et al. (Eds.), *Climate change in continental isotopic records, Geophysical Monograph 78*. Washington, DC, USA: American Geophysical Union. https://doi.org/10.1029/GM078p0001

Sano, M., Xu, C., & Nakatsuka, T. (2012). A 300-year Vietnam hydroclimate and ENSO variability record reconstructed from tree ring $\delta^{18}O$. *Journal of Geophysical Research*, *117*, D12115. https://doi.org/10.1029/2012JD017749

Scholl, M. A., Shanley, J. B., Zegarra, J. P., & Coplen, T. B. (2009). The stable isotope amount effect: New insights from NEXRAD echo tops, Luquillo Mountains, Puerto Rico. *Water Resources Research*, *45*, W12407. https://doi.org/10.1029/2008WR007515

Sime, L. C., Wolff, E. W., Oliver, K. I. C., & Tindall, J. C. (2009). Evidence for warmer interglacials in East Antarctic ice cores. *Nature*, *462*(7271), 342–345. https://doi.org/10.1038/nature08564

Singh, H. K. A., Bitz, C. M., Donohoe, A., Nusbaumer, J., & Noone, D. C. (2016). A mathematical framework for analysis of water tracers. Part II: Understanding large-scale perturbations in the hydrological cycle due to CO_2 doubling. *Journal of Climate*, *29*(18), 6765–6782. https://doi.org/10.1175/JCLI-D-16-0293.1

Smith, R. B., & Evans, J. P. (2007). Orographic precipitation and water vapor fractionation over the southern Andes. *Journal of Hydrometeorology*, *8*(1), 3–19. https://doi.org/10.1175/JHM555.1

Sodemann, H., Masson-Delmotte, V., Schwierz, C., Vinter, B. M., & Wernli, H. (2008). Interannual variability of Greenland winter precipitation sources: 2. Effects of North Atlantic Oscillation variability on stable isotopes in precipitation. *Climate Dynamics*, *113*(D12), D12111. https://doi.org/10.1029/2007JD009416

Sturm, C., Zhang, Q., & Noone, D. (2010). An introduction to stable water isotopes in climate models: Benefits of forward proxy modelling for paleoclimatology. *Climate of the Past*, *6*(1), 115–129. https://doi.org/10.5194/cp-6-115-2010

Sutanto, S. J., Hoffmann, G., Worden, J., Scheepmaker, R. A., Aben, I., & Röckmann, T. (2015). Atmospheric processes governing the changes in water isotopologues during ENSO events from model and satellite measurements. *Journal of Geophysical Research: Atmospheres*, *120*, 6712–6729. https://doi.org/10.1002/2015JD023228

Tierney, J. E., Russell, J. M., Huang, Y., Sinninghe Damsté, J. S., Hopmans, E. C., & Cohen, A. S. (2008). Northern Hemisphere controls on tropical southeast African climate curing the past 60,000 years. *Science*, *322*(5899), 252–255. https://doi.org/10.1126/science.1160485

Torri, G., Ma, D., & Kuang, Z. (2017). Stable water isotopes and large-scale vertical motions in the tropics. *Journal of Geophysical Research: Atmospheres*, *122*, 3703–3717. https://doi.org/10.1002/2016JD026154

Wright, J. S., Sobel, A. H., & Schmidt, G. A. (2009). Influence of condensate evaporation on water vapor and its stable isotopes in a GCM. *Geophysical Research Letters*, *36*, L12804. https://doi.org/10.1029/2009GL038091